


# Analysis of Corrosion Rate of Nanohybrid AA 6351/SiC/ZrO<sub>2</sub> Composites by Tafel Extrapolation Technique

T. SarithNaidu<sup>1</sup>  · K. VenkataSubbaiah<sup>1</sup>

Received: 15 July 2023 / Accepted: 4 October 2023  
© The Institution of Engineers (India) 2023

**Abstract** The corrosion resistance of an aluminium alloy (AA 6351) reinforced with nano-Silicon Carbide particles and various weight ratios of nano-Zirconium dioxide particles is explored in this study. AA6351–nanoSiC (5 wt%) composites were treated using powder metallurgy to add nanoZrO<sub>2</sub> (3–9 wt% in steps of 3%) to the composition. Electrochemical polarisation measurements assessed the effect of nano-Zirconium dioxide reinforcement on corrosion behaviour in a 3.5% sodium chloride solution. The Tafel method calculated the corrosion rate and the achieved polarisation results. Thus, according to findings, adding more nano-Zirconium dioxide particles into the aluminium alloy (6351) +5% SiC matrix increase corrosion resistance and decrease corrosion rate.

**Keywords** Aluminium alloy 6351 · Corrosion rate · Powder metallurgy · Hydraulic pellet press · NaCl · Corrosion current density · Tafel plot

## List of Symbols

AA	Aluminium alloy
$I_{\text{corr}}$	Corrosion current density
$E_{\text{corr}}$	Corrosion potential
$R_p$	Polarization resistance
$\beta_a$	Anodic slope (Volts/Decade)
$\beta_c$	Cathodic slope (Volts/Decade)
CR	Corrosion rate (mm/year or mils per year)
OCP	Open circuit potential
EIS	Electrochemical impedance spectroscopy

SEM	Scanning electron microscopy
ZrO <sub>2</sub>	Zirconium dioxide or zirconia
SiC	Silicon carbide
BPR	Ball to powder ratio
ASTM	American society for testing and materials
HANMMC	Hybrid aluminium nanometal matrix composite
PM	Powder metallurgy
SEM	Scanning electron microscope
AMC	Aluminium matrix composite
BN	Boron nitride
ZrB <sub>2</sub>	Zirconium diboride
Si <sub>3</sub> N <sub>4</sub>	Silicon nitride
EDS	Energy dispersive spectroscopy

## Introduction

Due to their future use in automobiles, ships, offshore constructions, and marine environments [1, 2], a small number of aeroplanes, helicopters, and spacecraft-spatial framework [3, 4] and LNG carriers and pressure vessels, aluminium alloy composites are valuable materials. Recent studies were intrigued by aluminium metal matrix composites because they coupled strong corrosion resistance with strength, low density, low wear rate, good thermal stability and a minimal cost of production [5]. The alignment and dispersion of the reinforced particles, as well as manufacturing methods such as stir casting, squeeze casting, ultrasonic-assisted stir casting, and powder metallurgy [6, 7], all significantly affect the physical and mechanical properties of the aluminium metal matrix composite. The particulate reinforcements are most favourable due to the reduction in nano-size from micro-size particles, allowing for improved morphological, physical, and mechanical characteristics. Al<sub>2</sub>O<sub>3</sub> [8], Graphite, B<sub>4</sub>C

✉ T. SarithNaidu  
infosarith@andhrauniversity.edu.in

<sup>1</sup> Department of Mechanical Engineering, Andhra University, Visakhapatnam 530003, India

[9], MWCNT [7], SiC [5, 10, 11], TiB<sub>2</sub> [12–14], TiC [15, 16], ZrO<sub>2</sub> [17], Flyash [18], AlN [19], ZrB<sub>2</sub>, and Si<sub>3</sub>N<sub>4</sub> are currently widely utilised as reinforcement to the base material in a bid to enhance mechanical characteristics. Due to its potential to produce products with a near-net-like form and its ability to achieve a good degree of reinforcing homogeneity in the composite material, powder metallurgy garnered the most interest amongst the many fabrication techniques for AMCs. As a result, the expensive manufacturing operations are reduced, which makes the production process cost-effective [17].

A better alternative to mono-reinforced composites, hybrid composites enhanced with a blend of micro-, nano-sized or nano–nano-sized particles, had additionally drawn scientific study focus [13]. This is owing to their superior physico-mechanical characteristics. Nanosized particles empower the matrix function better because of the Orowan strengthening process.

Using traditional powder metallurgy procedures, the effects of Silicon Carbide grain size (11, 6, and 3 μm) and volume fraction (up to 15% vol%) on the microstructure and corrosion behaviour of Aluminium metal matrix composite strengthened by silicon carbide were investigated by Zakaria [20]. The corrosion rate of the Aluminium MMC reinforced with SiC is reduced by decreasing the grain size and/or raising the percentage volume of silicon carbide grains. At 50 and 75 °C, the composite samples corroded faster than the pure Aluminium.

The corrosion properties were tested on Al7075/TiC and [21] Al6061/SiC with 10 and 20 wt% particles by the Tafel method—one of the electrochemical analyses in a 3.5 M sodium chloride medium. The specimen's microstructure displayed pits, and pits grew as NaCl concentration increased [16].

Thiagarajan et al. [22] investigated the WEDM process parameters of Al6061-reinforced composites made of nanoSiC and nanoZrO<sub>2</sub> through stir casting. The aluminium matrix was strengthened with hybrid nano-powders, producing a tough material. Zirconia (ZrO<sub>2</sub>) nanoparticles offer excellent reinforcement for aluminium matrices due to their physical, mechanical, and wear properties. The blend of micro- and nanoSiC (5 wt%) and nano-Zirconia with various weight percentages (3, 6, and 9) is analysed for improving the tribological and mechanical characteristics of aluminium matrices [14, 23, 24] by powder metallurgy technique. The wear surface of pure aluminium and hybrid composites was analysed using Scanning electron microscopy and ANOVA.

[25] Investigated the corrosion resistance by salt spray corrosion test according to ASTM B117 observed for one day in NaCl (3.5%) solution on samples of AA6061 reinforced with TiB<sub>2</sub> particles (2.5–7.5 wt% in steps of 2.5) produced by an in-situ process. The corrosion rate decreases, or corrosion resistance increases with an increase in TiB<sub>2</sub>

particles. The optimum corrosion rate of 1.4815 miles/year is obtained for AA6061/TiB<sub>2</sub> at 7.5 wt% TiB<sub>2</sub>.

The corrosion rate of Al6061 alloy and its composite with reinforcements are distinguished by two approaches—weight loss and electrochemical methods in acid and neutral chloride medium [26–28]. There is a slight difference between the corrosion rates obtained by the two approaches because the composite was exposed to the electrolyte for longer when weight loss measurements were made [28].

Karthikeyan [29] studied the corrosion properties of the Aluminium alloy 8011 strengthened with TiC (10 and 20 wt%) Gr (1 & 2 wt%) through electrochemical methods like OCP, cyclic polarisation resistance and EIS, and observed that the corrosion rate decreases with increased TiC, whereas adding Graphite reduces the corrosion resistance. [30] Studied the potentiodynamic polarisation technique for calculating the corrosion resistance of an alloy of aluminium alloy 2024 reinforced with ZrO<sub>2</sub> nanoparticles of varied weight percentages (0, 2, 4 and 6%) prepared by Stir casting. Including ZrO<sub>2</sub> nanoparticles greatly improves the corrosion resistance of the aluminium metal matrix composite in a seawater environment.

Joel Hemanth et al. [31]: probed the corrosion behaviour of NanoZirconia of particle size 100–200 nm reinforced with LM-13 composites in a 3.5% NaCl solution by electrochemical method for aerospace application. Due to the nanoscale zirconia in ZrO<sub>2</sub>, the findings at 3, 6, 9 and 12 weight percent show that these composites have superior corrosion resistance than LM-13 alloy.

Prasannanagasai et al. [32] developed AA 7075 reinforced ZrO<sub>2</sub> particles (2 and 4 wt%) made by stir casting to examine the wear, mechanical, and electrochemical corrosion properties. Due to the excellent bonding of the ZrO<sub>2</sub> reinforcement in AA 7075 alloy, corrosion resistance is enhanced at 2 and 4 wt% ZrO<sub>2</sub> reinforced composites.

Sukriti Yadav [33] investigated the mechanical and corrosion characteristics of the hybrid aluminium nanocomposites reinforced with 1–3 weight percent of each silicon carbide, graphite, and ZrO<sub>2</sub> through a stir casting technique. Aluminium reinforced with one wt% each of SiC/ZrO<sub>2</sub>/Gr, i.e. at 3 wt%, was analysed in 3.5% NaCl solution at ambient temperature by the Tafel method had the maximum corrosion resistance.

In addition to being inexpensive and readily available, zirconium dioxide is a mineral metal oxide with excellent fracture toughness and wear properties. After reviewing the relevant literature, no detailed dissertation on nanoZrO<sub>2</sub>-strengthened AA6351 and nano-silicon carbide composites fabricated via the powder metallurgy method is available. Hence, powder metallurgy is utilised to develop hybrid aluminium nanometal matrix composites for hull structures, bicycle frames, and marine and aerospace applications. The microstructural analysis of

samples has been performed, and the corrosion behaviour of nanohybrid SiC+ZrO<sub>2</sub> aluminium alloy composites has been investigated by the electrochemical(Tafel) method in 3.5% NaCl solution.

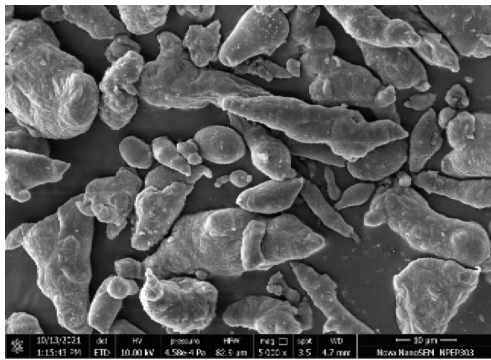
### Experimental Details

#### Fabrication of Composites

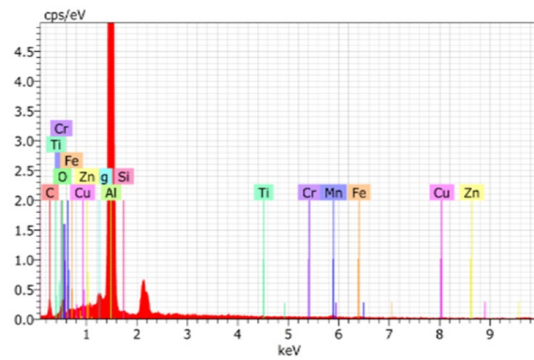
Aluminium alloy (6351) (Parshwamani metals, Mumbai), silicon carbide, and zirconium dioxide powders (Nano-Research laboratories, India) with average sizes of 70–80 μm and 30–50 nm particles, respectively, were acquired. Figure 1a–d displays the SEM images of the particles as they were received. For the study, the composition, as mentioned below, of nanocomposites is concocted using the powder metallurgy method.

S. No	Sample	Composition (wt%)		
		AA	SiC	ZrO <sub>2</sub>
1)	SAZ1	100	0	0
2)	SAZ2	95	5	0
3)	SAZ3	92	5	3
4)	SAZ4	89	5	6
5)	SAZ5	86	5	9

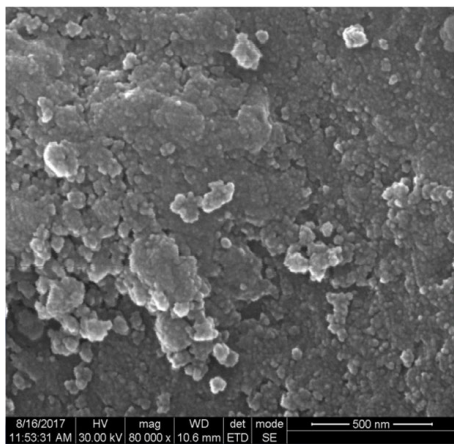
Initially, the weight of the enlisted powders was computed with a digital balance (AS R220 plus, Swiss Manufactured, ES 225SM-DR) with a minimum count of 0.1 mg. A preset quantity of nanoSiC (3.21 g/cm<sup>3</sup>), nanoZrO<sub>2</sub> (5.68 g/cm<sup>3</sup>), and aluminium alloy 6351 powder (2.71 g/cm<sup>3</sup>) was profoundly blended Using a planetary ball mill (VBCRC, Chennai) with steel balls of dia 8 mm, and a 10:1 BPR was used to reduce the agglomeration of composite powders during blending for 30 min at a speed of 125 rpm. The characterisation of these milled blended powders is conducted on XRD (Bruker D8) to know the presence of various elements



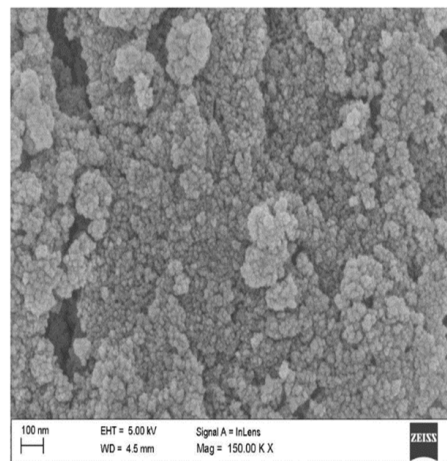
a) AA6351 SEM image



b) EDS Report AA 6351



c) SEM images of ZrO<sub>2</sub> nanoparticles



d) Silicon Carbide nanoparticles

Fig. 1 a–d SEM images of AA6351, SiC and ZrO<sub>2</sub>

in each blend, functioning with a wavelength of  $1.5418 \text{ \AA}$  using  $\text{CuK}\alpha$  X-rays at 30 kV with a range ( $2\theta$ ) of  $20^\circ$ – $80^\circ$  and  $0.02^\circ$  step size. The obtained graph was validated with Match! Software. [17]. Pellets with a size of 13 mm dia and 5 mm thick were produced at a rate of 3 tonnes utilising a 20-tonne automated hydraulic pellet press (VBCRC, Chennai) for the sintering operation muffle furnace (VBCRC, Chennai). To ensure good die operation, the die surface was manually wiped and greased with zinc stearate for every compression process. The specimens were sintered at  $550^\circ\text{C}$  for 1 h in a muffle furnace and cooled to room temperature in the furnace chamber.

### Sample Preparation for Microstructure

The samples were sequentially ground, polished, etched, and examined under an optical microscope. Wet grinding with water uses SiC emery paper with different grits (220, 320, 500, and 1000). The sample is thoroughly cleaned to remove any remaining grit and swart before changing each grit and polishing paper. Polishing is carried out on a rotating wheel with select cloth and alumina powder in grades ranging from 1 to  $2 \mu\text{m}$ . The sample is polished until it has a mirror finish. Polishing leaves a thin layer of amorphous metal on the sample's surface. This layer is known as the flowed layer, and it covers deep scratches, cavities, small non-metallic particles, and the sample's proper structure. The flowed layer can be removed entirely by etching when the etching process is done to the samples using an etchant of 99%  $\text{H}_2\text{O}$  + 1% HF. The suitability of its polishing surface is observed on a microscope before it is processed further to etching to get exemplary microstructures. Leica Microscope was used to inspect the samples optically and sample images for corrosion are shown in Fig. 5a–e.

### Electrochemical Testing Method

Corrosion studies were conducted in Sodium chloride salt solution using approximately 13 mm diameter and 5 mm thick Aluminium alloy 6351 and hybrid aluminium nanometal matrix composite samples as shown in Fig. 3. Before the corrosion test, all five samples were polished with emery sheets of various grades until the samples had a mirror surface finish. The electrochemical corrosion test uses Vertex. C (IVIUM) workstations. The setup of the electrochemical test consists of aluminium alloys as working electrodes with a cross-sectional area of  $1.0 \text{ cm}^2$ , Ag/AgCl as an electrode for reference, and a thin platinum wire as an auxiliary electrode. As shown in Fig. 2, functional electrodes were developed by coupling an insulated copper wire to one side of the specimen by sealing it with aluminium conducting tape and cold mounting it in epoxy resin. The electrode arrangements are as per ASTM G 102 standards [34].

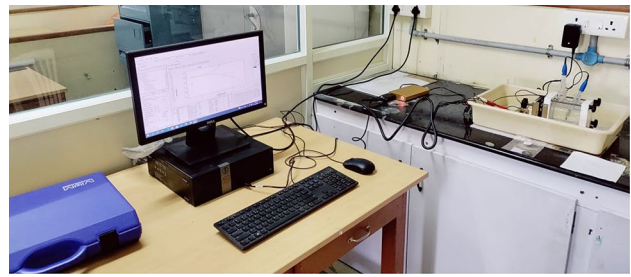


Fig. 2 Apparatus for polarisation test

## Results & Discussion

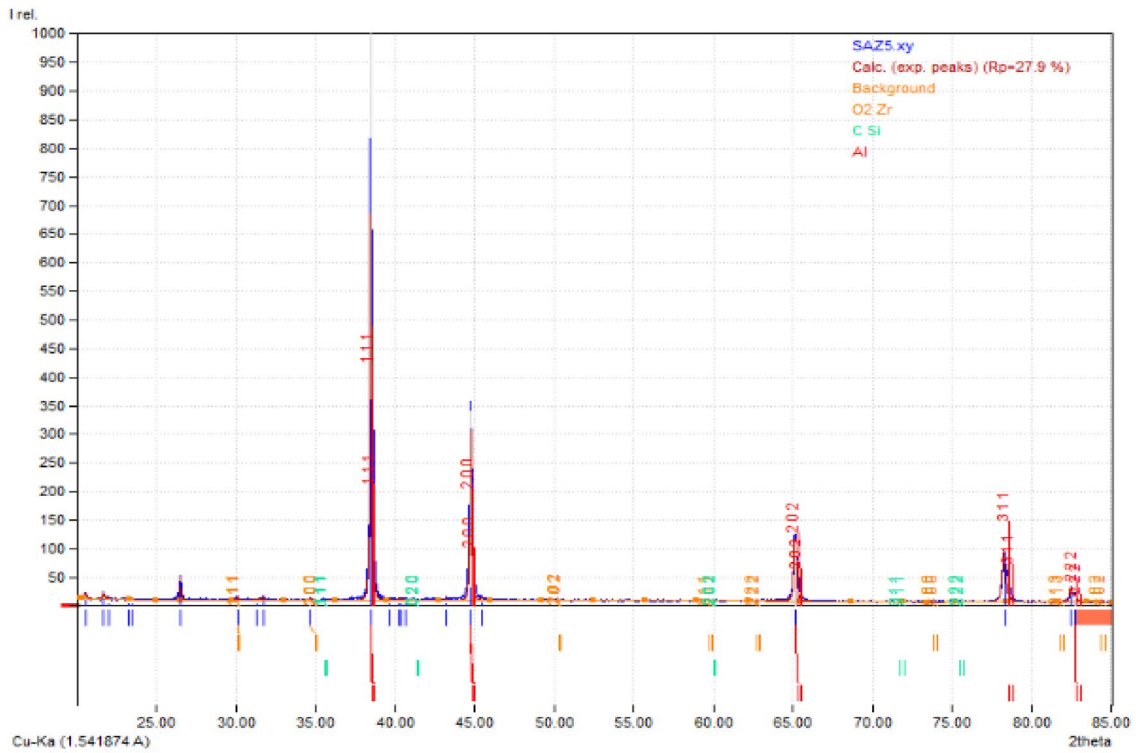
### X-ray Diffraction

Figure 3 shows the XRD pattern of the sample powders—SAZ2 (AA 6351 + 5 wt% SiC), SAZ3 (AA 6351 + 5 wt% SiC + 3 wt%  $\text{ZrO}_2$ ), SAZ4 (AA 6351 + 5 wt% SiC + 6 wt%  $\text{ZrO}_2$ ) and SAZ5 (AA 6351 + 5 wt% SiC + 9 wt%  $\text{ZrO}_2$ ) prepared by planetary ball mill for 30 minutes. The Aluminium peak is the largest observed at  $38.45^\circ$ . The XRD graph of the samples is valid with Match Software with Crystallography Open Database-CIF (crystallography information file) 9010158 for SiC [35], 1502689 for Aluminium [36] and 5000038 for  $\text{ZrO}_2$  [37]. X-ray Diffraction analysis reveals the peaks and phases of Aluminium, SiC and  $\text{ZrO}_2$  combinations which is good agreement with the literature [24]. Figure 4 illustrates the energy dispersive spectroscopy (EDS) investigation of the produced composite. The EDS analysis reveals distinct peaks corresponding to elements such as Aluminium, Silicon, Zirconium, Magnesium, Zinc, C, Fe, and O, Cu and Ti all of which are discernible in the depicted graph (Fig. 5), which confirms the homogeneous dispersion of the nanohybrid reinforcements (SiC and  $\text{ZrO}_2$ ) in

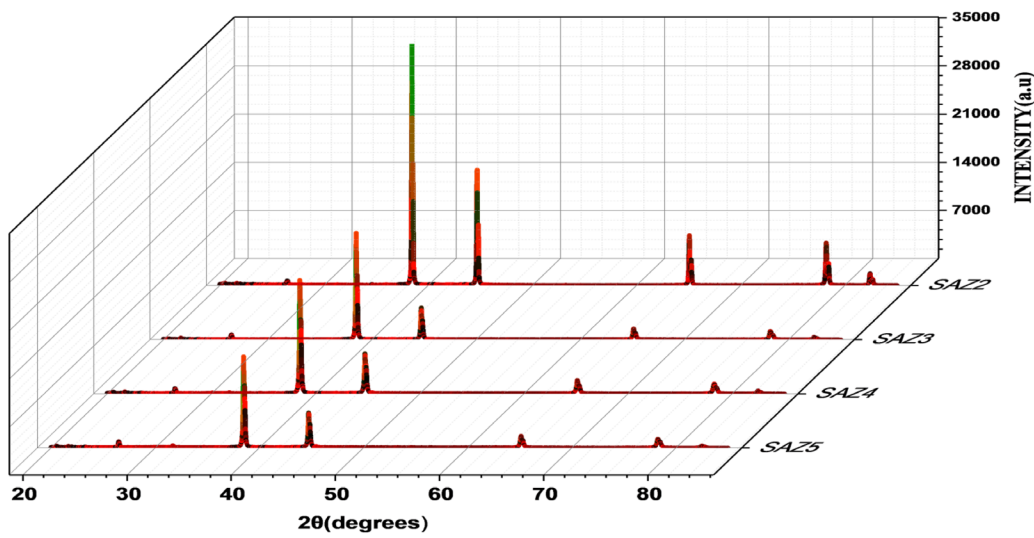
### Tafel Plot

Electrochemical tests include potentiostatic holds, cyclic anodic polarisation, and open circuit potential monitoring. Figure 6 displays the Tafel polarisation curves for AA6351 and hybrid aluminium nanocomposite reinforced with nanoSiC and various weight percentages of zirconium dioxide nanoparticles 3–9 wt% in steps of 3 wt% in a 3.5% sodium chloride medium. These graphs show that the corrosion behaviour of all samples in a 3.5% NaCl solution exhibits identical cathodic and anodic polarisation curves. However, the five samples' corrosion current density and potential (SAZ1, SAZ2, SAZ3, SAZ4, and SAZ5) varied. In a different cell, open circuit potential observations were made for 20 min. The potentiodynamic polarisation behaviour of aluminium alloys in the potential range of  $-1$



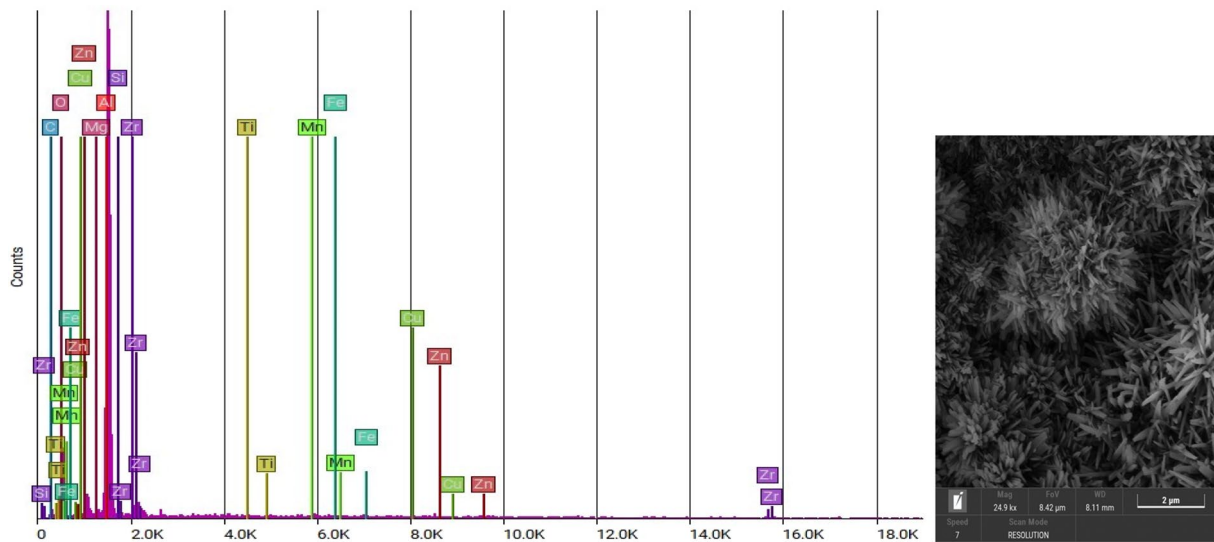


a) XRD of SAZ5- hybrid nanocomposites made from the base metal alloy AA 6351 and 5wt% nanoSiC and 9 wt% nanoZrO<sub>2</sub>- Match software



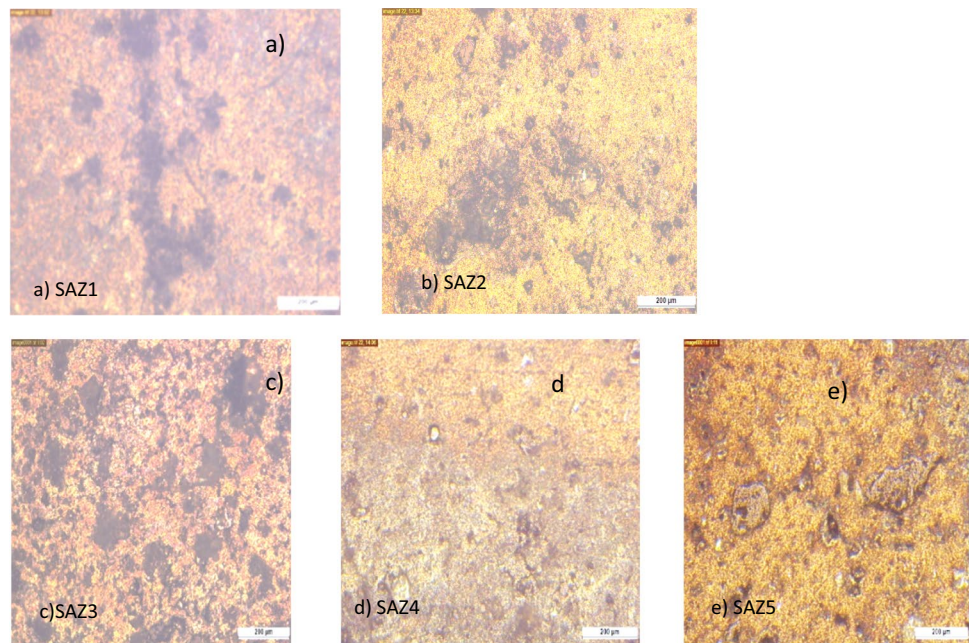
b) XRD of SAZ2, SAZ3, SAZ4 AND SAZ5

Fig. 3 a–b XRD samples



**Fig. 4** SAZ5 -SEM-EDS of AA6351++ 5 wt% SiC+9 wt% ZrO<sub>2</sub> nanocomposites

**Fig. 5 a–e** Optical microstructure of AA6351 and HANMMC after corrosion



to +1.5 V s at room temperature is obtained using a sweep rate of 10 mV/sec to calculate the corrosion current density, corrosion potential and the corrosion rate (CR). The polished specimens were sterilised with water and acetone to eliminate any possible surface elements that could have deposited and influenced the measurement after each experiment, and the electrolyte was replenished. After finding signs of the initial pitting on the potentiodynamic curve, the testing was halted.

The Tafel curves were produced using the log of the corrosion current density to the potential. A linear zone has been seen in the tafel extrapolation close to the  $E_{\text{corr}}$  on both

the cathodic and anodic extremities. The Tafel constants  $\beta_a$  and  $\beta_c$  represent the slopes of the linear regions. These linear zones are extrapolated until they cross to produce  $E_{\text{corr}}$  [26]. Corrosion current density is determined by the log  $I_{\text{corr}}$  values at the coordinates' intersection. Figure 6 shows the Tafel polarisation curves of the all the five samples (SAZ1-aluminium alloy 6351, SAZ2-aluminium alloy reinforced with nanoSiC and SAZ3, SAZ4, SAZ5-hybrid nanocomposites made from the base metal alloy AA 6351 and 5 wt% nanoSiC and nanoZrO<sub>2</sub>) in 3.5 wt%NaCl solution. The Tafel curves demonstrate that a hybrid composite's corrosion rate descends as the weight percentage of nanozirconia

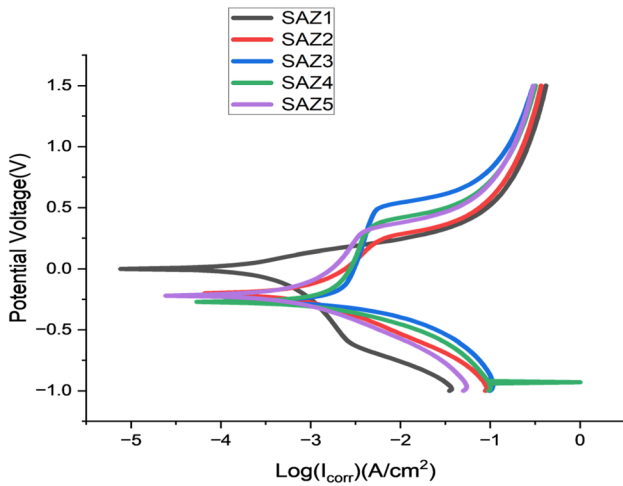


**Fig. 6** Tafel plot of pure aluminium alloy, aluminium alloy reinforced with SiC and HANMMC with varied wt% of ZrO<sub>2</sub>

accelerates. Compared to three weight percent nanoZrO<sub>2</sub>, the hybrid composite’s Tafel plot at nine wt% nanoZrO<sub>2</sub> exhibits the steepest anodic slope and lower I<sub>corr</sub> current; hence, it is corrosion resistant. The electrochemical variables such as anodic and cathodic slope (Volts/Decade), corrosion current density, corrosion potential, R<sub>p</sub> Polarisation resistance (Ω cm<sup>2</sup>) and Corrosion rate (mpy or mm/yr) are obtained from the Tafel extrapolation curve as depicted in Table 1. This illustrates that with the increase in nano-ZrO<sub>2</sub> from 3 to 9 wt% in the AA6351/SiC, the corrosion rate descends from 0.7440 to 0.1331 mm/yr or 29.333 to 5.2451 mpy as depicted in Fig. 7, and thus, SAZ5 has excellent resistance to corrosion in 3.5% sodium chloride solution. Zirconia and SiC are inert ceramic particles that the corrosion may scarcely impact, which may explain the enhanced corrosion resistance.

**Computation of Rate of Corrosion**

$$CR = \frac{K1 \times \text{Equivalent Weight} \times I_{corr}}{\rho} \tag{1}$$

where CR is mm/year or mils/ year, I<sub>corr</sub> (corrosion current density (μA/cm<sup>2</sup>)) is the ratio of the corrosion current

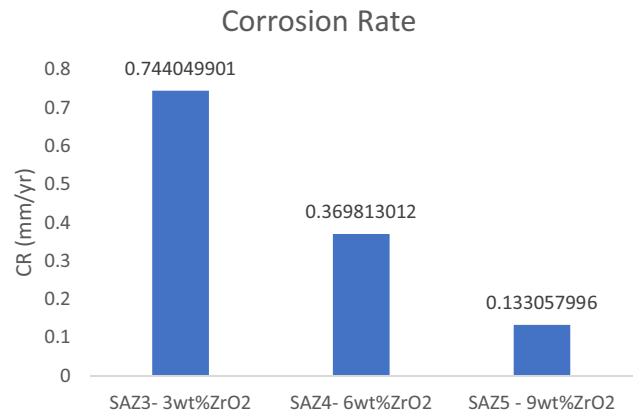


**Fig. 7** HANMMC with varied wt% of ZrO<sub>2</sub>

(i<sub>corr</sub>) to the sample area (1sqcm) &(ρ) density of the aluminium alloy and its hybrid reinforced composites (g/cm<sup>3</sup>) and K1 = 3.27 × 10<sup>-3</sup> mm g/μA cm y or 0.129 mpy g/μA cm. Sample equivalent weight is considered dimensionless. Table 1 displays the rate of corrosion for AA 6351 and its hybrid aluminium nanocomposites in 3.5% NaCl, calculated using the above Eq. (1) [34].

**Conclusions**

The main objective of this thesis is to study the corrosion performance of the nanohybrid metal matrix composite with varying weight percentages (3–9 in steps of 3) of nano-zirconium dioxide added to the base aluminium alloy6351 and nanoSiC.

- The effect of adding five weight percent nanoSiC to the AA6351 and with various amounts of nano-zirconium dioxide reinforced to aluminium alloy 6351 and nanoSiC prepared by powder metallurgy was analysed to find the corrosion rate by an electrochemical method like Tafel extrapolation method in NaCl medium for applications like hull structures, bicycle frames, marine and aerospace sectors.
- X-ray Diffraction analysis and SEM–EDS confirms the presence of SiC and ZrO<sub>2</sub> reinforcement in the alumin-

**Table 1** Corrosion rate

Sample	Tafel slope (V/dec)		R <sub>p</sub> (Ω cm <sup>2</sup> )	I <sub>corr</sub> (A/cm <sup>2</sup> )	Corrosion potential (V)	Corrosion rate	
	Anodic	Cathodic				mm/yr	mpy
SAZ1	0.132	0.174	3044	1.07E−05	0.0054	0.1179	4.64701
SAZ2	0.239	0.184	1045	4.33E−05	−0.208	0.472996324	18.64967228
SAZ3	0.223	0.092	408.3	6.92E−05	−0.1462	0.744049901	29.33327058
SAZ4	0.133	0.056	489.8	3.495E−05	−0.2819	0.369813012	14.5800317
SAZ5	0.1	0.069	1386	1.28E−05	−0.226	0.133057996	5.245163207

ium alloy6351. Microstructure revealed a pitting form of corrosion on the material surfaces.

- The corrosion rate of the composites investigated can be formed in a descending order as: SAZ3 < SAZ4 < SAZ5. The corrosion resistance of the three nanohybrid metal matrix composite samples in descending order is: SAZ5 < SAZ4 < SAZ3 which clearly denotes that increasing the weight percentage of the Zirconium dioxide has improved the corrosion resistance of hybrid aluminium nanometal matrix composite. Despite of aluminium alloy6351 exhibits the excellent resistance, it is further concluded that SAZ5 showing an excellent resistance to corrosion in 3.5% NaCl solution which will be suitable for the applications like hull structures, bicycle frames, marine and aerospace sectors.

**Author Contributions** All authors contributed to the study conception and design. Material preparation, data collection and analysis were performed by KV and TS. The first draft of the manuscript was written by TS and all authors commented on previous versions of the manuscript. All authors read and approved the final manuscript.

**Funding** The authors declare that no funds, grants, or other support were received during the preparation of this manuscript.

**Data Availability** All data used to support the findings of this study are included within the article.

#### Declarations

**Conflict of interest** The authors confirm that this article's content has no conflict of interest.

**Ethics Approval** Not applicable.

**Consent to Participate** Not applicable.

**Consent for Publication** The authors declare that the figures and tables used in this manuscript are original and are not published anywhere.

## References

1. B. Baudouy, A. Four, Low temperature thermal conductivity of aluminum alloy 5056. *Cryogenics* **60**, 1–4 (2014). <https://doi.org/10.1016/j.cryogenics.2013.12.008>
2. P. Sharma, S. Sharma, K. Dinesh, A study on the microstructure of the aluminium matrix composites. *J Asian Cer Soci* **3**, 240–244 (2015)
3. P.C. McDonald et al. (2006) Thermal validation of the design of the CFRP support struts to be used in the spatial framework of the Herschel Space Observatory. *Cryogenics*. 46298-304
4. N. Jagadeesh, A.P. Senthil-Kumar, S. Janaki, Studies on mechanical and thermal behaviors of Al6061-SiC-Gr-ZrO<sub>2</sub> nanohybrid composites. *Mater. Res. Expr.* (2018). <https://doi.org/10.1088/2053-1591/aadb6f6>
5. O. El-Kady, A. Fathy, Effect of SiC particle size on the physical and mechanical properties of extruded Al matrix nanocomposites. *Mater. Des.* **54**, 348 (2014)
6. K. Sekar, G. Jayachandra, S. Aravindan, Mechanical and welding properties of A6082-SiC-ZrO<sub>2</sub> hybrid composite fabricated by stir and squeeze casting. *Mater. Today Proc.* **5**, 20268–20277 (2018)
7. P.S. Samuel Ratna Kumar, D.S. Robinson Smart, S. John Alexis, Corrosion behaviour of aluminium metal matrix reinforced with multi-wall carbon nanotube. *J Asian Cer Societ* **5**, 71–75 (2017)
8. A. Baradeshwaran, A.E. Perumal, Study on mechanical and wear properties of Al7075/Al<sub>2</sub>O<sub>3</sub>/graphite hybrid composites. *Comp. Part B* **56**, 464–471 (2014)
9. A. Baradeshwaran, S.C. Vettivel, A.E. Perumal, N. Selvakumar, R.F. Issac, Experimental investigation on mechanical behaviour, modelling and optimization of wear parameters of B<sub>4</sub>C and graphite reinforced aluminium hybrid composites. *Mater. Design* **63**, 620–632 (2014)
10. K.S. Shetty, A.N. Shetty, Studies on corrosion behavior of 6061 Al-15 vol. pct. SiC(p) composite in HCl Medium by electrochemical Techniques. *Surf. Eng. Appl. Electrochem.* **51**, 374–381 (2015)
11. S. Arif, M.T. Alam, T. Aziz, H.A. Ansari, Morphological and wear behaviour of new Al–SiC micro-SiC nano hybrid nanocomposites fabricated through powder metallurgy. *Mater. Res. Expr.* **5**, 046534 (2018). <https://doi.org/10.1088/2053-1591/aabcf0>
12. R. Sharma, A.K. Singh, A. Arora, S. Pati, P.S. De, Effect of friction stir processing on corrosion of Al-TiB<sub>2</sub> based composite in 35 wt% sodium chloride solution. *Trans. Nonferr. Met. Soc. China* **29**(7), 1383–1392 (2019). <https://doi.org/10.1016/S1003-6>
13. T. Aoshuang, T. Jie, Z. Xiang, F. Dingfa, Z. Hui, Fabrication of aluminium hybrid reinforced with SiC microparticles and TiB<sub>2</sub> nanoparticles by powder metallurgy. *Powder Metall.* **60**, 66–72 (2017)
14. S. Arif, M.T. Alam, A.H. Ansari, M.B. Shaikh, M.A. Siddiqui, Analysis of tribological behaviour of zirconia reinforced Al-SiC hybrid composites using statistical and artificial neural network technique. *Mater. Res. Expr.* **5**, 056506 (2018). <https://doi.org/10.1088/2053-1591/aabec8>
15. S. Kumar, A. Kumar, C. Vanitha, Corrosion behaviour of Al 7075/ TiC composites processed through friction stir processing. *Mater. Today Proc.* **15**, 21–29 (2019). <https://doi.org/10.1016/j.matpr.2019.05.019>
16. E.S.M. Sherif, H.S. Abdo, K.A. Khalil, A.M. Nabawy, Effect of titanium carbide content on the corrosion behavior of Al-TiC composites processed by high energy ball mill. *J. Electrochem. Sci. Int.* (2016). <https://doi.org/10.20964/2016.06.18>
17. S. Arif, T. Aziz, A.H. Ansari, Characterization and mechanical behaviour of zirconia reinforced aluminium matrix nanocomposites fabricated through powder metallurgy technique. *Mater. Focus* **7**(6), 901–905 (2018). <https://doi.org/10.1166/mat.2018.1612>
18. M.B.N. Shaikh, S. Arif, M.A. Siddiqui, Fabrication and characterization of aluminium hybrid composites reinforced with fly ash and silicon carbide through powder metallurgy. *Mater. Res. Expr.* **5**, 046506 (2018)
19. S.K. Selvaraj, M.K. Nagarajan, L.A. Kumaraswamidhas, An investigation of abrasive and erosion behavior of AA 2618 reinforced with Si<sub>3</sub>N<sub>4</sub>, AlN and ZrB<sub>2</sub> in situ composites by using optimization techniques. *Arch. Civil Mech. Eng.* **17**, 43–54 (2017). <https://doi.org/10.1016/j.acme.2016.08.003>
20. H.M. Zakaria, Microstructural and corrosion behavior of Al/SiC metal matrix composites. *Ain Shams Eng. J.* **5**, 831–838 (2014)
21. M.K. Abbass, K.S. Hassan, A.S. Alwan, Study of corrosion resistance of aluminum alloy 6061/SiC composites in 3.5% NaCl solution. *Int. J. Mater. Mech. Manuf.* **3**, 31–35 (2015). <https://doi.org/10.7763/IJMMM.2015.V3.161>



22. C. Thiagarajan, T. Maridurai, T. Shaafi, A. Muniappan, Machinability studies on hybrid nano-SiC and nano-ZrO<sub>2</sub> reinforced aluminium hybrid composite by wire-cut electrical discharge machining. *Mater. Today: Proceed.* (2021). <https://doi.org/10.1016/j.matpr.2021.07.029>
23. A. Khan, M.W. Abdelrazeq, M.R. Mattli, M.M. Yusuf, A. Alashraf, P.R. Matli, R.A. Shakoor, Structural and mechanical properties of Al-SiC-ZrO<sub>2</sub> nanocomposites fabricated by microwave sintering technique. *Crystals* **10**, 904 (2020). <https://doi.org/10.3390/cryst10100904>
24. S. Arif, M.T. Alam, A.H. Ansari, M.A. Siddiqui, M. Mohsin, Study of mechanical and tribological behaviour of Al/SiC/ZrO<sub>2</sub> hybrid composites fabricated through powder metallurgy technique. *Mater. Res. Expr.* **4**, 076511 (2017). <https://doi.org/10.1088/2053-1591/aa7b5f>
25. S. Chandrasekhara, N.B.V. Prasad, Experimental investigation on mechanical, wear and corrosive properties of Aa6061-Tib2 in-situ composites produced by K2tif6- Kbf4 reaction system at optimum holding time. *AIP Conf. Proc.* **2327**, 020037 (2021). <https://doi.org/10.1063/5.0039805>
26. N. Sunitha, K.G. Manjunatha, S. Khan, M. Sravanthi, Study of SiC/graphite particulates on the corrosion behavior of Al 6065 MMCs using tafel polarization and impedance. *SN Appl. Sci.* (2019). <https://doi.org/10.1007/s42452-019-1063-6>
27. S. Khan, K.G. Manjunatha, Comparisons of pitting corrosion characteristics of Al6061matrix alloy and its composite by weight loss and electrochemical method. *Int. J. Res. Aeronaut. Mech. Eng.* **6**(1), 1–16 (2018)
28. J.A. Kamaj, Comparison of potentiodynamic polarization and weight loss measurements techniques in the study of corrosion behavior of 6061 Al/SiC composite in 3.5 M NaCl solution. *Asian J. Appl. Sci.* **3**, 264–270 (2015)
29. A. Karthikeyan, G.R. Jinu, Investigation on mechanical and corrosion behaviour of AA8011 reinforced with TiC and graphite hybrid composites. *Mater. Res. Expr.* **6**, 1065b5 (2019). <https://doi.org/10.1088/2053-1591/ab3e87>
30. E. Kennedy, B.S. Sachin, M. Ramachandra, C.A. Niranjana, N. Sriraman, V.K. Jain, N.S. Narayanan, Effect of ZrO<sub>2</sub> nano-particles on mechanical and corrosion behaviour of Al2024 alloy. *Mater. Today: Proceed.* (2020). <https://doi.org/10.1016/j.matpr.2020.06.194>
31. J. Hemanth, M.R. Divya, Fabrication and corrosion behaviour of aluminium alloy (LM-13) reinforced with Nano-ZrO<sub>2</sub> particulate chilled nano metal matrix composites (CNMMCs) for aerospace applications. *J. Mater. Sci. Chem. Eng.* **6**, 136–150 (2018). <https://doi.org/10.4236/msce.2018.67015>
32. P.N. Bellamkonda, S. Sudabathula, V. Mohan Srikanth, A. Rajesh, Wear and electrochemical corrosion behaviour of nano ZrO<sub>2</sub> reinforced aa7075 metal matrix composites. *Int. J. Mech. Prod. Eng. Res. Develop* **9**(3), 793–802 (2019)
33. S. Yadav, S. Gangwar, P.C. Yadav, V.K. Pathak, S. Sahu, Mechanical and corrosion behavior of SiC/Graphite/ZrO<sub>2</sub> hybrid reinforced aluminum-based composites for marine environment. *Surf. Topogr. Metrol. Prop.* **9**, 045022 (2021). <https://doi.org/10.1088/2051-672X/ac2f87>
34. ASTM G102: Practice for calculation of corrosion rates and related information from electrochemical measurements
35. C.L. Burdick, E.A. Owen, The atomic structure of carborundum determined by x-rays. *Am. Chem. Soc.* **40**(12), 1749–1759 (1918). <https://doi.org/10.1021/ja02245a001>
36. F.M. Mulder, B. Assfour, J. Huot, T.J. Dingemans, M. Wage-maker, A.J. Ramirez-Cuesta, Hydrogen in the metals. *J. Phys. Chem. C* **114**, 10648 (2010)
37. U. Martin, H. Boysen, F. Frey, Neutron powder investigation of tetragonal and cubic stabilized zirconia, TZP and CSZ, at temperatures up to 1400 K. *Acta Cryst.* **B49**, 403–413 (1993). <https://doi.org/10.1107/S0108768192011297>

**Publisher's Note** Springer Nature remains neutral with regard to jurisdictional claims in published maps and institutional affiliations.

Springer Nature or its licensor (e.g. a society or other partner) holds exclusive rights to this article under a publishing agreement with the author(s) or other rightsholder(s); author self-archiving of the accepted manuscript version of this article is solely governed by the terms of such publishing agreement and applicable law.